Origin of Structural Inhomogeneities in Polymer Gels

Eriko Sato Matsuo,† Michal Orkisz,‡ Shao-Tang Sun,§ Yong Li,∥ and Toyoichi Tanaka*,‡

Department of Applied Biological Sciences and Department of Physics and Center for Materials Science and Engineering, Massachusetts Institute of Technology, Cambridge, Massachusetts 02139, Hercules, Inc., Wilmington, Delaware 19894, and Kimberly-Clark, Inc., Neenah, Wisconsin 54956-0056

Received April 13, 1993; Revised Manuscript Received August 10, 1994•

ABSTRACT: The structure of a cross-linked polymer network depends not only on its chemical constituents but also on the conditions under which the gel is polymerized. Highly nonuniform spatial distributions of polymer network concentration and cross-linking density are observed in most polymer gels. The inhomogeneities, as studied using light scattering, are shown to result from two origins: one from the dynamic critical fluctuations of the polymer solution at the onset of gelation, and the other from the domain formation due to the microphase separation. Both are directly related to the phase equilibrium properties of the gel during the gelation process. Those fluctuations of polymer density are frozen in the gel structure permanently. In addition to these permanent spatial fluctuations, a polymer network undergoes thermal dynamical concentration fluctuations which diverge at the critical point. These three types of fluctuations, two static and one dynamic, account for the nature of gel inhomogeneities. The static spatial fluctuations reversibly increase and diverge at the spinodal line, although they are permanent inhomogeneities. A qualitative interpretation is given to account for this phenomenon.

Introduction

The formation of heterogeneous structures of cross-linked polymer gels has been the subject of great interest for many years, since the physical properties of gels are directly affected by the degree of heterogeneities in gels. The structural inhomogeneities of a gel affect greatly its physical properties such as permeability, elasticity, and optical and phase properties. Extensive studies have been made on the characterization of the gel inhomogeneities. Weiss and Silberberg showed that high permeability of acrylamide gels is related to the inhomogeneous cross-link distribution.[1,2] Hsu and colleagues examined the effects of inhomogeneities of the polymer network on the swelling equilibrium of acrylamide gels and on the diffusion of water molecules within the gels.[3] The ring structures and intramolecular chemical reactions during gelation were studied by Standford and Stepto.[4] They found that the shear moduli of the polyester and polyurethane gels were reduced markedly in the presence of such elastically ineffective polymer network loops. Funke reviewed several different polymer networks with nonuniform distributions of cross-links.[5] The groups of Candau and Geissler quantified the inhomogeneities using various neutron, X-ray, and static light scattering techniques and proposed models explaining the difference between gels and equivalent solutions.[6,7]

The parameters used commonly to vary the network structure and its inhomogeneities are the concentration of polymers and the proportion of cross-linkers to polymers. For polyacrylamide gels, Richards and Temple described a model which relates gel compositions with the swelling ratio, turbidity, elastic modulus, and volume fractions.[8] Bansil and Gupta determined the boundary between a clear state and an opaque, heterogeneous state for a gel as a function of monomer and cross-linker concentrations.[9] Nishio and co-workers compared gels prepared at two different temperatures and qualitatively described the difference.[10]

It is well-known that the turbidity of a gel is a direct result of light scattered from the spatial inhomogeneities of its refractive index.

Dusek proposed a model of microsyneresis, where a dispersion of separated pure liquid phase and the remaining gel structure is responsible for the scattering of light.[11] In this paper, we present a more general picture for the physical principle underlying the formation of spatial inhomogeneities in polymer gels. From examinations of the effects of gelation temperature on the spatial distribution of polymer network density using quasielastic and elastic light scattering techniques, we conclude that there are three types of causes for the structural inhomogeneities within a gel. First, the dynamic concentration fluctuations of pregel polymer solutions are frozen in the final network structure upon the onset of the gelation process. Second, if the polymer solution is in the phase separation regime, there appear two gel phases having two different concentrations. The domain sizes of these two phases depend on the condition of the gelation process and can sometimes have a size order of the wavelength of light and scatter light tremendously giving strong opacity to the gel.[11] In both cases the phase equilibrium properties of the gel play an essential role in determining the permanent structural inhomogeneities within a gel. Third, in addition to having these permanent structural inhomogeneities, a gel undergoes temporal thermal concentration fluctuations. These inhomogeneities give an opacity to a gel similar to the critical opalescence of binary fluids. These dynamic concentration fluctuations have been previously investigated using the technique of quasielastic light scattering.[12–15] See also a recent discussion by Geissler in ref 16.

Extensive studies of dynamic and static light scattering from gels with various chemical compositions showed the presence of inhomogeneous structures embedded within the polymer networks and their influence on dynamic properties of the gels.[11,16] The permanent inhomogeneities contribute to the phenomenon of nonergodicity of a gel, which attracted much attention from experimentalists and theorists.[16–22]

† Department of Applied Biological Sciences, MIT.
‡ Department of Physics and Center for Materials Science and Engineering, MIT.
§ Hercules, Inc.
∥ Kimberly-Clark, Inc.
• Abstract published in *Advance ACS Abstracts*, October 1, 1994.

0024-9297/94/2227-6791$04.50/0

Experiments

Sample Preparation. The gels were formed by free radical copolymerization of *N*-isopropylacrylamide (7.8 g) and *N,N'*-methylenebisacrylamide (0.130 g) in 100 mL of deionized water. Tetramethylethylenediamine (TEMED, 240 μL) and ammonium persulfate (43 mg) were used as accelerator and initiator, respectively. Prior to the gelation the pregel solution was filtered using a 0.22 μm filter, degassed in vacuo, and then transferred into a micropipet for gelation. The temperature of the gelation process was controlled by immersing the micropipets containing the samples into a circulating heat bath. The gels thus prepared had the lower critical point at approximately 34 °C.

The light scattering cells used in the experiments were 100 μL glass micropipets (1.31 mm inner diameter) placed inside optical square cuvettes of 1 cm inner side filled with water (for room temperature measurements) or in a sample holder with a thermoelectric device for temperature control.

Light Scattering. In order to quantify the inhomogeneities of the gel network structure, we determined the scattered light intensity and the intensity autocorrelation function at an angle of 90° using a microscopic laser light scattering (MLLS) setup. An incident beam (632 nm) from a He–Ne laser (Spectra Physics 127) was coupled into a single-mode optic fiber and then focused to the center of the cylindrical scattering cell with a beam waist of the order of 10 μm. The sample cell was mounted on a microscope stage, which could be moved perpendicularly to the scattering plane. In a typical experiment the sample cell was moved every 7.5 μm using a stepping motor. The scattered light intensity and the intensity autocorrelation function (collected with a Brookhaven BI-2030AT correlator with 136 linear channels) were determined simultaneously at each position at various temperatures. In the measurement of temperature dependence experiments the temperature of the sample cell was controlled to within 0.01 °C. (The gelation temperature dependence experiments were run at room temperature.)

The samples were gels exhibiting a large degree of nonergodicity; so they had to be analyzed as such. A lot of recent literature has been devoted to the question of light scattering from nonergodic media. The seminal paper of Pusey and van Megen[18] laid out the theoretical foundations for such analysis, which was later successfully applied to gels.[20-22] Fang et al.[21] give a summary and comparison of various methods applicable to nonergodic media.

The approach pursued by these authors is to evaluate the ensemble-averaged correlation function on the basis of the time-average correlation function collected at a single point and of the ensemble-averaged intensity (which is much simpler to obtain than the correlation function). In this paper a more "brute force" approach was taken. Raw correlation functions were measured at N different locations obtained by laterally translating the sample. We used $N = 50$ for measurement temperature and $N = 150$ for gelation temperature dependence. It has been observed that in our MLLS setup the intensities measured at two points further than 5 μm apart were uncorrelated. Therefore a step size of 7.5 μm between consecutive points was employed. The raw correlation functions were then summed and normalized, forming an approximation $g_N^{(2)}(t)$ to the ensemble average $g_E^{(2)}(t)$. The clear disadvantage of this method is that a large number of correlation functions must be obtained. This is offset by the fact that each of them can be collected over a period N times shorter than the single time-averaged measurement mentioned above, while the sum maintains the proper statistical accuracy. Another question is what value of N is large enough to adequately represent the ensemble average. Let I be a random variable corresponding to the spatial distribution of the time-invariant intensity. It obeys a power law distribution (due to a Gaussian distribution of the corresponding electric field[18]). It can be easily verified that the standard deviation is equal to the square of the average $\langle I \rangle$. Summing N such random variables gives, by the Central Limit Theorem, a random variable with a relative deviation of $1/N^{1/2}$. So, for $N = 50$ and $N = 150$ we obtain standard deviations of, respectively, 14.1% and 8.2%.

It is well-known (the Siegert relationship) that for an electric field whose ensemble distribution is a zero-mean Gaussian variable one can write

$$g_E^{(2)}(t) - 1 = \beta |g^{(1)}(t)|^2$$

where $g^{(1)}(t) = \langle E_p(\tau) \cdot E_p^*(\tau + t) \rangle_E / \bar{I}$ is the normalized ensemble-averaged electric field correlation function, while β is an instrumental parameter due to spatial integration of the speckle pattern over a finite detector area. It was determined experimentally to be 0.8 by repeating the scattering experiment with the same geometry but using an ergodic medium (polystyrene latex spheres).

To extract further information from the correlation function, a simple model was used which assumed the electric field autocorrelation function to be a sum of a single-exponentially decaying dynamic and constant static components:

$$|g^{(1)}(t)| = (\bar{I}_D/\bar{I}) e^{-Dq^2 t} + (\bar{I}_S/\bar{I})$$

Here $\bar{I}_D$ and $\bar{I}_S$ are the ensemble-averaged dynamic (fluctuating) and static intensities, D is the diffusion constant, and q is the scattering vector. One observes that $|g^{(1)}(t)| = 1$ at $t = 0$ and $(\bar{I}_S/\bar{I})$ as $t \to \infty$. In order to correct for finite N and for the instrumental parameter β, we form a quantity

$$G_\infty^2 \equiv 1 - \{g_N^{(2)}(0) - g_N^{(2)}(\infty)\}/\beta = (\langle I_S \rangle_N / \langle I \rangle_N)^2$$

where $\langle ... \rangle_N$ denotes an average over N points. Having independently measured $\langle I \rangle_N$ we then recover

$$\langle I_S \rangle_N = \langle I \rangle_N G_\infty$$

$$\bar{I}_D = \langle I \rangle_N (1 - G_\infty)$$

The diffusion coefficient D is actually obtained by fitting $g_N^{(2)}(t)$ with a single exponential $Ae^{-D^* q^2 t} + B$ and then correcting D^* for heterodyning of $\bar{I}_D$ with $\langle I_S \rangle_N$.

Results

General Observations. The positional dependence of the scattered light intensity measured at room temperature is shown in Figure 1. The scattered light intensity of the gel made at 20 °C fluctuates substantially as the scattering position is scanned within the gel. It is important to observe that the fluctuation profile is reproducible when measurements are repeated along the same path along the gel, as shown in the figure (in agreement with ref 22). This indicates that the light scattering is from a structure that is restricted in the gel rather than from dynamic fluctuations. If the scattering were due to the dynamical fluctuations of the polymer network, the scattering intensity would not depend on the position within the gel, because the scattering intensity is an average over a time period much longer compared to the fluctuation time. The intensity of the scattered light did not become zero even when it was at a minimum value. This further confirms the validity of the analysis proposed above where the residual intensity $\bar{I}_D$ originates from light scattered by the dynamic collective mode of the polymer network and is present at every point within the gel.

Figure 2 depicts a typical $g_N^{(2)}(t)$ curve obtained by summing and then normalizing the raw correlation functions obtained at each point. Also shown is a curve corrected for finite N and for the instrumental parameter β according to

$$G^2(t) \equiv 1 - \{g_N^{(2)}(0) - g_N^{(2)}(t)\}/\beta$$

As described above, the values of $\langle I_S \rangle_N / \langle I \rangle_N$ and $\bar{I}_D / \langle I \rangle_N$ can be easily read from $G^2(\infty)$. A fit of the function $A(e^{-t/\tau} + R)^2 + B$ to the corrected curve is also shown. Two points should be mentioned. As seen from the residuals, the quality of the fit is indeed excellent. However, the analysis

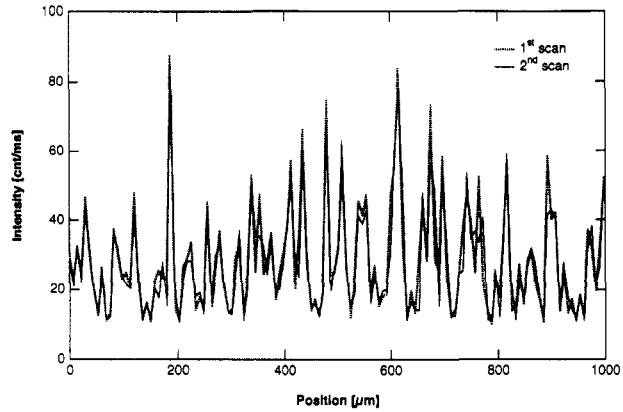

Figure 1. Position dependence of scattered light intensity from an *N*-isopropylacrylamide gel, prepared at 20 °C. Positions were changed in 7.5 μm steps using a motor. Two measurements were carried out along the same measurement paths to show the permanency and reproducibility of the profile of light intensity scattered from gel inhomogeneities.

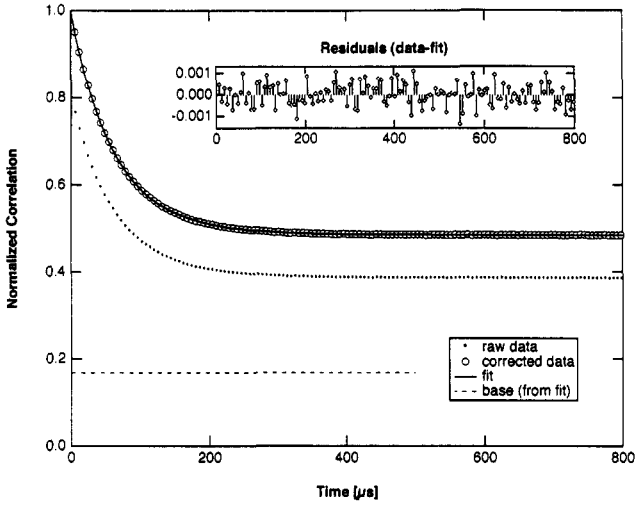

Figure 2. Typical autocorrelation curve (dots) obtained by summing and then normalizing the raw correlation functions obtained at each point. Also shown (open circles) is this curve corrected for finite N and for the instrumental parameter β. The solid line is a fit of $A(e^{-t/\tau} + R)^2 + B$ to this curve. The dashed line shows B for this fit. The residuals are plotted in the insert.

presented above assumes $B = 0$, whereas a positive value is obtained from the fit (indicated as the dashed line on the graph). This is most easily explained by the presence of light which is incoherent with the dynamic part; thus it does not take part in the heterodyning, though it contributes to the total intensity. In such a case our analysis would lump it with the $\bar{I}_S$, introducing only a small error to the overall result.

Dependence on Gelation Temperature. The scattered light intensity fluctuations are strongly dependent on the temperature at which the gels were made. As shown in Figure 3a–c, the amplitude of the fluctuations increased substantially as the gelation temperature was increased. The results are summarized in Figure 4. Both $\bar{I}_S$ and $\bar{I}_D$ are plotted as a function of the temperature at which gelation takes place. All measurements were carried out at room temperature. For the gels made at low temperatures the average intensities, $\bar{I}_S$ and $\bar{I}_D$, were low. However, $\bar{I}_S$ increased as the gelation temperature increased and seemed to jump quite drastically around 28 °C. The gels made above this temperature showed a permanent translucence, turning to opacity at even higher temperatures. It should be noted that the polymerization of *N*-isopropylacrylamide is an exothermic reaction; so the actual gelation temperature might have been slightly higher than the temperature of the heat bath which is reported here. $\bar{I}_D$ remained almost constant, decreasing only at high temperatures. The diffusion coefficient D plotted in Figure 6a is practically independent of the gelation temperature, even at the high end.

Dependence on Measurement Temperature. The position dependence of scattered light intensity of an *N*-isopropylacrylamide gel made at 20 °C was determined as a function of measurement temperature. The results are shown in the right half of Figure 3d–f and summarized in Figure 5. Both $\bar{I}_S$ and $\bar{I}_D$ are plotted as a function of the temperature at which gelation takes place. In the figure the inverses of these intentisites are also plotted. As the temperature approached the critical temperature of 33.4 °C, the static ($\bar{I}_S$) and dynamic ($\bar{I}_D$) amplitudes increased and appeared to diverge. The divergence of the dynamic amplitude can be understood as the critical divergence of the density fluctuations of the polymer network. This was confirmed by observing the collective diffusion coefficient of the gel, which showed critical slowing down at the same temperature (Figure 6b).[13]

Discussion

Generally, one would not need to invoke the frozen concentration fluctuations to explain the positional fluctuation of the scattered intensity in Figures 1 and 3. It can result from the restricted motion of the scatterers.[18] However, the data on gelation temperature dependence strongly suggest the existence of frozen concentration fluctuations. In the limiting case of a translucent or opaque gel we know explicitly that their size is at least on the order of the wavelength of light. The fact that $\bar{I}_S$ increases strongly with rising gelation temperature can be interpreted as an effect of larger and larger clusters being formed during the gelation process (see below). The fact that $\bar{I}_D$ and the diffusion coefficient D remain unaffected would indicate that the dynamic fluctuations are due to chains connecting the clusters. Furthermore, the perfect fit by a single exponential in Figure 2 confirms the applicability of the collective diffusion theory to these portions of the gel. The decrease of $\bar{I}_D$ at high gelation temperatures, coinciding with the samples becoming translucent, could be accounted for by the onset of multiple scattering and/or saturation of the photomultiplier tube at high intensity. But it could also be interpreted as a decrease in the fraction of chains not bound within the clusters.

The origin of the frozen concentration fluctuations can be understood from the schematic phase diagram, as shown in Figure 7, where the horizontal axis indicates the polymer network density and the vertical axis shows the reduced temperature (corresponding to Flory–Huggins interaction parameter[23]). Note that the reduced temperature of *N*-isopropylacrylamide gels is a monotonically decreasing function of temperature. For a binary system consisting of polymers and solvent, the phase boundary is dependent on the molecular weight of the polymer.[23] At the early stage of the gelation process, the effective molecular weight of the polymer is small. The phase boundary of such a system is relatively symmetric with the critical concentration located near 50%. As the polymerization proceeds, the effective molecular weight of the polymer increases. The phase boundary moves; the critical reduced temperature decreases and so does the critical concentration. When the gelation threshold is reached, the evolution of the phase boundary in the phase diagram stops. The dynamic fluctuations of the polymer solution will then be frozen in space and give rise to the spatial concentration

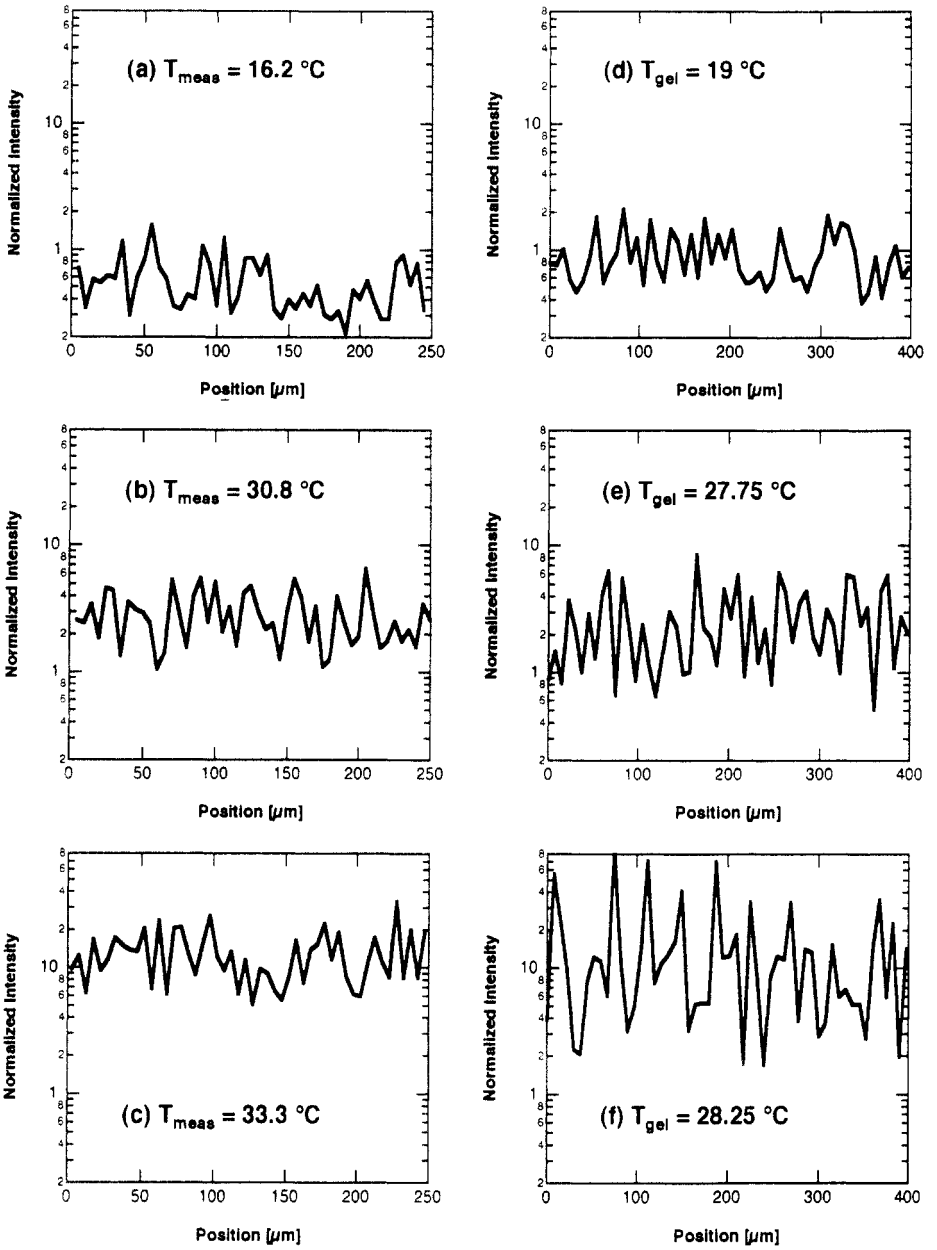

Figure 3. Position dependence of light intensity scattered from an *N*-isopropylacrylamide gel shown as a function of gelation temperature (a–c). The measurement temperature was 23 °C. On the right side of the figure (d–f), the position dependence of scattered light intensities is shown for different measurement temperatures, but for a fixed gelation temperature of 20 °C.

fluctuations within the gel. The inhomogeneities of the gel structure are then uniquely characterized by the correlation length of dynamic fluctuations at the onset of gelation. This correlation length is determined by the relative location of the state point in the phase diagram with respect to the phase boundary at the gelation. For gels prepared at high reduced temperatures (for example, point A in Figure 7), the phase boundary is well below this state point, which ensures small fluctuations and a uniform gel structure. The gel made in such a condition is very clear. In contrast, the gels made at lower reduced temperatures (points B and C in Figures 7) are more inhomogeneous as a result of the increasingly strong dynamical concentration fluctuations, since the state point is near the phase boundary and the precritical behavior emerges. The static concentration fluctuations appear to critically diverge at 33.4 °C.

It is important to notice that although the structural inhomogeneities are permanently embedded within the polymer network, their amplitude, or the contrast between dense and dilute regions, is enhanced as the gel approaches the spinodal line. This phenomenon can be interpreted as follows. At equilibrium, the osmotic pressure within a gel is homogeneous. Due to the structural inhomogeneities, the isobar is different from place to place within the gel. The isobar for the entire gel is, therefore, represented by a blurred line, as illustrated in Figure 8. The distribution of polymer density is indicated by the intercept of the horizontal line at a fixed temperature and the blurred isobar. The distribution is finite far from the spinodal line but increases and diverges as the reduced temperature becomes that of a spinodal line. Namely, as the gel approaches the spinodal line, the originally denser regions become denser and the originally dilute regions become more dilute. This leads to a larger contrast in the refractive index fluctuations, and thus to a larger light scattering.

Conclusion

Using light scattering, we have studied the origin of structural inhomogeneities within a gel. There are two kinds of permanent structural inhomogeneities and dynamic fluctuations. All of these are determined by the relative position of the gel state point within the phase diagram either at the onset of the gelation process or at

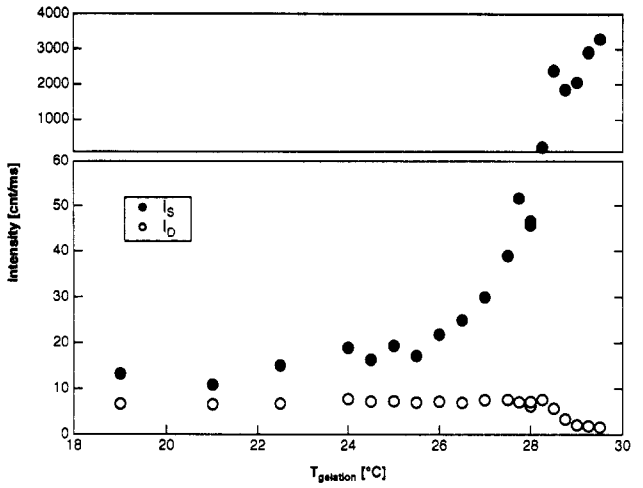

Figure 4. Amplitudes of the spatial ($\bar{I}_S$) and dynamic ($\bar{I}_D$) fluctuations of scattering intensity plotted as a function of the temperature at which the gel is prepared. The measurements were carried out at 23 °C. $\bar{I}_S$ appears to jump at 28 °C. $\bar{I}_D$ remains almost constant.

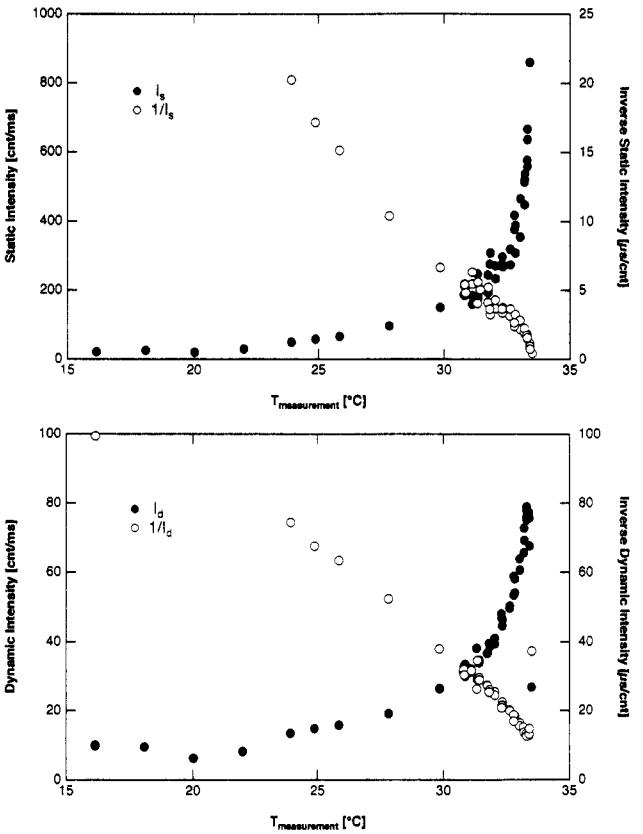

Figure 5. Amplitude $\bar{I}_S$ and its inverse of the spatial fluctuations of scattering intensity plotted as a function of the measurement temperature at which the light scattering was carried out (upper graph). The sample was made at 20 °C. The amplitude appears to diverge at 33.4 °C. The amplitude of dynamic fluctuations, $\bar{I}_D$, also diverges (lower graph).

the measurements of inhomogeneities. Therefore, the concept of phase transitions of the gel and polymer solution is important to predict the gel network structure. The spatial inhomogeneities, although their structure is permanent, can be enhanced as the temperature approaches the spinodal line and diverge at the line.

The findings and the concept presented here will be useful in controlling the gel structure and thus the physical properties of gels such as permeability, viscoelasticity, and optical clarity. Moreover, the studies presented here show that information may be stored in a distributed way as

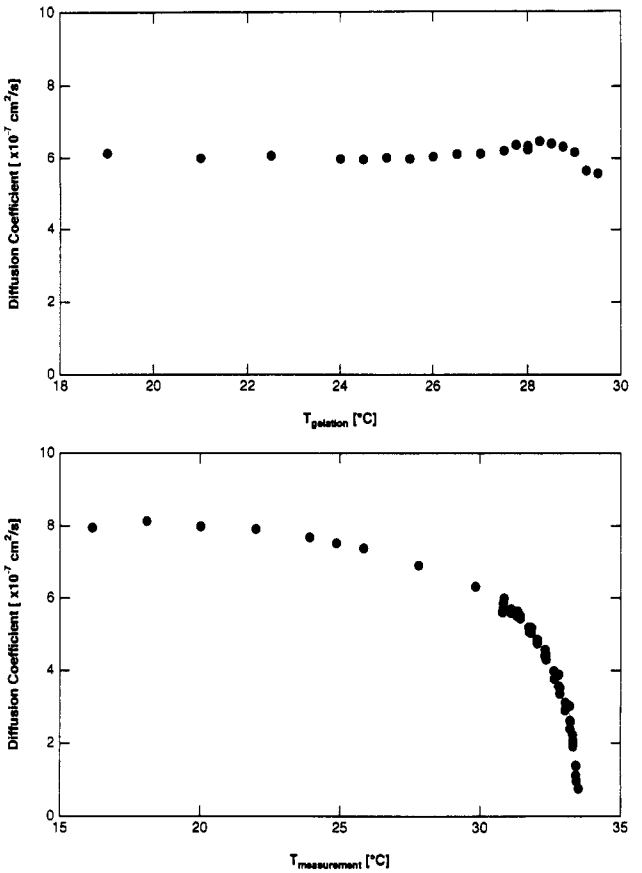

Figure 6. Collective diffusion coefficient of concentration fluctuations of *N*-isopropylacrylamide gel (as determined by quasielastic light scattering) plotted as a function of gelation temperature (upper graph) and of measurement temperature (lower graph). In the first case the measurements were carried out at 23 °C. In the second, the gel was prepared at 20 °C. In the lower graph the diffusion coefficient diminished at 33.4 °C, showing the critical slowing down.

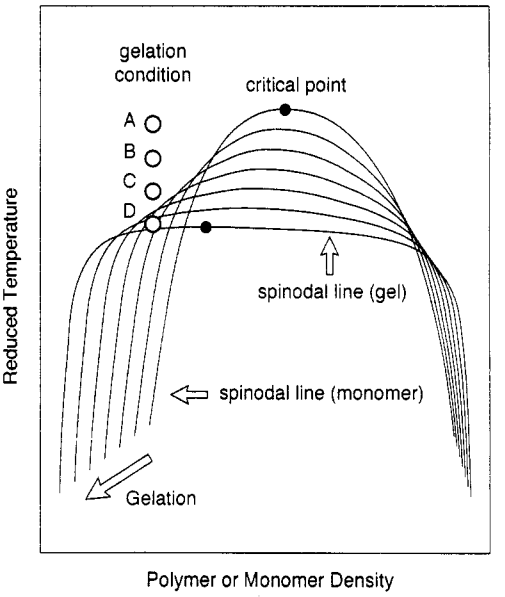

Figure 7. Schematic phase diagram of a gel and pregel solutions. The vertical axis corresponds to the reduced temperature, which is a monotonically decreasing function of temperature in the case of *N*-isopropylacrylamide gels. If gelation occurs far above the spinodal line, the gel is homogeneous and clear. If it ocurs near the spinodal line, the gel is translucent and less homogeneous. If it occurs within the spinodal line, the gel is completely opaque.

spatial inhomogeneities within the three-dimensional gel and that it can be readily observed by the angular dependence of scattered laser light. This may be useful

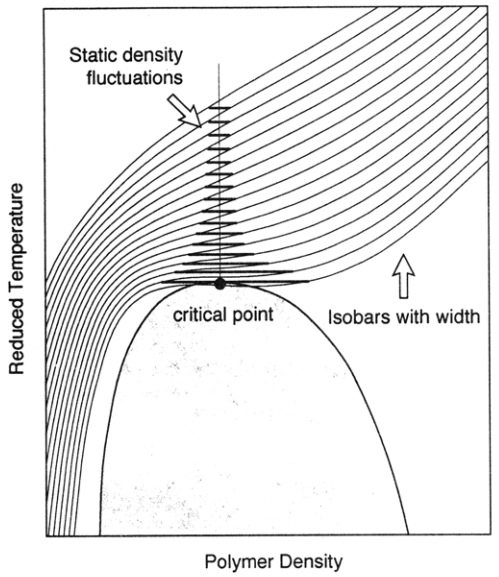

Figure 8. The isobar of a gel has a width due to the inhomogeneities within the gel. The density distribution is narrow far from the spinodal line but diverges at the line. This explains why the amplitude of spatial inhomogeneity increases and diverges at the spinodal line.

in various applications including three-dimensional holography.

There are several interesting unsolved questions concerning the inhomogeneities. For example, the discrepancy between the temperatures of divergence for static and dynamic scattering is not addressed here (but see ref 24). The inhomogeneities created near the gelation threshold are also an interesting problem. The study of these questions will lead us to a better understanding of the structure and properties of polymer gels.

Acknowledgment. Work was supported by the National Science Foundation, DMR 87-19217, and NIH-LBRC, P41-RR02594-09.

References and Notes

(1) Weiss, N.; Silberberg, A. *Polym. Prepr. (Am. Chem. Soc., Div. Polym. Chem.)* **1975**, *16* (2), 289.
(2) Weiss, N.; van Vliet, T.; Silberberg, A. *J. Polym. Sci., Polym. Phys. Ed.* **1974**, *17*, 2229.
(3) Hsu, T. P.; Ma, D. S.; Cohen, C. *Polymer* **1983**, *24*, 1273.
(4) Stanford, J. L.; Stepto, R. F. T. *Polym. Prepr. (Am. Chem. Soc., Div. Polym. Chem.)* **1981**, *22*, 165.
(5) Funke, W. *Plast. Rubber Process. Appl.* **1983**, *3*, 243.
(6) Hecht, A. M.; Duplessix, R.; Geissler, E. *Macromolecules* **1985**, *18*, 2167.
(7) Candau, S. J.; Ilmain, F.; Schosseler, F.; Bastide, J. *Mater. Res. Soc. Symp. Proc.* **1990**, *177*, 3.
(8) Richards, E. G.; Temple, C. J. *Nat. Phys. Sci.* **1971**, *230*, 92.
(9) Bansil, R.; Gupta, M. K. *Ferroelectrics* **1980**, *30*, 64.
(10) Suzuki, Y.; Nozaki, K.; Yamamoto, T.; Itoh, K.; Nishio, I. *J. Chem. Phys.* **1992**, *97*, 3808.
(11) Dusek, K. In *Polymer Networks*; Chompff, A. J., Newman, S., Eds.; Plennum: New York, 1971; pp 245–260.
(12) Tanaka, T. *Phys. Rev.* **1978**, *A17*, 763.
(13) Tanaka, T.; Ishiwata, S.; Ishimoto, C. *Phys. Rev. Lett.* **1977**, *38*, 771.
(14) Hockberg, A.; Tanaka, T. *Phys. Rev. Lett.* **1979**, *43*, 217.
(15) Munch, J. P.; Candau, S.; Duplessix, R.; Picot, C.; Herz, J.; Benoit. *J. Polym. Sci., Polym. Phys. Ed.* **1976**, *14*, 1097.
(16) Geissler, E. In *Dynamic Light Scattering*; Brown, W., Ed.; Oxford University Press: Oxford, U.K., 1993, pp 471–511.
(17) Goldbart, P.; Goldfeld, N. *Phys. Rev. Lett.* **1987**, *58*, 2676.
(18) Pusey, P. N.; van Megen, W. *Physica A* **1989**, *157*, 705.
(19) Chu, B. *Laser light scattering*; Academic Press: London, 1991.
(20) Joosten, J. G.; McCarthy, J. L.; Pusey, P. N. *Macromolecules* **1991**, *24*, 6690.
(21) Fang, L.; Brown, W. *Macromolecules* **1992**, *25*, 6897.
(22) Skouri, R.; Munch, J. P.; Schosseler, F.; Candau, S. J. *Europhys. Lett.* **1993**, *23*, 635.
(23) Flory, P. J. *Principles of Polymer Chemistry*; Cornell University Press: Ithaca, NY, 1953; pp 495–540.
(24) Rabin, Y.; Onuki, A. To be published.